Available online at www.sciencedirect.com

SCIENCE DIRECT®

Earth and Planetary Science Letters 228 (2004) 325–341

EPSL

www.elsevier.com/locate/epsl

Zircon geochronology and ca. 400 Ma exhumation of Norwegian ultrahigh-pressure rocks: an ion microprobe and chemical abrasion study

D.B. Root[a,*], B.R. Hacker[a,1], J.M. Mattinson[a,1], J.L. Wooden[b,2]

[a]*Department of Geological Sciences, University of California at Santa Barbara, Santa Barbara, CA 93106-9630, USA*
[b]*U.S. Geological Survey, 345 Middlefield Road, Menlo Park, CA 94025-3591, USA*

Received 3 December 2003; received in revised form 28 September 2004; accepted 11 October 2004
Available online 21 November 2004
Editor: K. Farley

Abstract

Understanding the formation and exhumation of the remarkable ultrahigh-pressure (UHP) rocks of the Western Gneiss Region, Norway, hinges on precise determination of the time of eclogite recrystallization. We conducted detailed thermal ionization mass spectrometry, chemical abrasion analysis and sensitive high-resolution ion-microprobe analysis of zircons from four ultrahigh- and high-pressure (HP) rocks. Ion-microprobe analyses from the Flatraket eclogite yielded a broad range of apparently concordant Caledonian ages, suggesting long-term growth. In contrast, higher precision thermal ionization mass spectrometry analysis of zircon subject to combined thermal annealing and multi-step chemical abrasion yielded moderate Pb loss from the first (lowest temperature) abrasion step, possible minor Pb loss or minor growth at 400 Ma from the second step and a 407–404 Ma cluster of slightly discordant $^{206}Pb/^{238}U$ ages, most likely free from Pb loss, from the remaining abrasion steps. We interpret the latter to reflect zircon crystallization at ~405–400 Ma with minor discordance from inherited cores. Zircon crystallization occurred at eclogite-facies, possibly post-peak conditions, based on compositions of garnet inclusions in zircon as well as nearly flat HREE profiles and lack of Eu anomalies in zircon fractions subjected to chemical abrasion. These ages are significantly younger than the 425 Ma age often cited for western Norway eclogite recrystallization, implying faster rates of exhumation (>2.5–8.5 km/Myr), and coeval formation of eclogites across the UHP portion of the Western Gneiss Region.

Keywords: zircon; U/Pb; UHP; REE; eclogite; Norway

* Corresponding author. Now at Department of Mineral Sciences, National Museum of Natural History, Smithsonian Institution, Washington, DC 20560-0119, USA. Tel.: +1 202 633 1815; fax: +1 202 357 2476.

E-mail addresses: rootd@si.edu (D.B. Root), hacker@geol.ucsb.edu (B.R. Hacker), mattinson@geol.ucsb.edu (J.M. Mattinson), jwooden@usgs.gov (J.L. Wooden).

[1] Fax: +1 805 893 2314.

[2] Fax: +1 650 329 4664.

0012-821X/$ - see front matter © 2004 Published by Elsevier B.V.
doi:10.1016/j.epsl.2004.10.019

1. Introduction

The Scandinavian Caledonides contain one of the largest tracts of high-pressure (HP) to ultrahigh-pressure (UHP) rocks in the world, and as such form an important natural laboratory for studying aborted continental subduction. The core of this large tract of continental rocks, the Western Gneiss Region, was subducted to depths of >135 km and subsequently exhumed to crustal levels at 390–385 Ma, based on white mica $^{40}Ar/^{39}Ar$ ages from the Nordfjord area [1].

Salient characteristics of the UHP and HP rocks within the Western Gneiss Complex have been described by Wain [2] and Cuthbert et al. [3], who mapped distinct HP and UHP provinces within Western Norway (Fig. 1). The UHP province contains eclogites with unzoned major element profiles and eclogite-facies inclusions in garnet, as well as coesite or coesite pseudomorphs, whereas eclogites from the HP province contain neither coesite nor coesite pseudomorphs, and prograde-zoned garnets with amphibolite-facies inclusions; these two zones are separated by a mixed HP/UHP zone which shares characteristics of both.

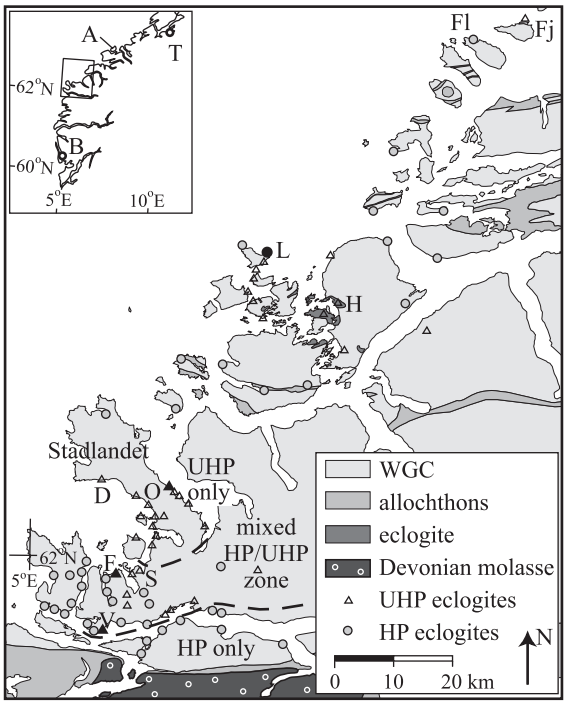

Fig. 1. Map of western Norway, including field area and all UHP locales. Filled symbols: samples from this study. UHP/HP boundaries adapted from Wain [2]. WGC—Western Gneiss Complex, A—Averøya, B—Bergen, D—Drage, F—Flatraket, Fj—Fjørtoft, Fl—Flemsøya, H—Hareidland, L—Langenes, O—Otnheim, S—Saltaneset, T—Trondheim, V—Verpeneset.

2. Geochronological background

The age of the Western Gneiss Region high-pressure metamorphism has been investigated by the Sm/Nd, U/Pb and U–Th/Pb methods. Griffin and Brueckner [4] obtained Sm/Nd mineral-whole-rock isochrons ranging from 407 to 447 Ma (Table 1), and averaged five of their Sm/Nd garnet-clinopyroxene isochrons to obtain an age of 425 Ma. However, this average may not have geological significance as all of the isochrons were obtained using only two points (at least three isotopic ratios are required to assess isotopic equilibrium). Moreover, the five ages, and their uncertainties, do not form a single statistical population. Subsequently, four other Sm/Nd ages of ~410 Ma have been reported by Mearns [5], Jamtveit et al. [6], Mørk and Mearns [7] and Carswell et al. [8], but the Silurian age has remained entrenched in the literature [9,10]. The 40 Myr range in Sm/Nd ages may reflect spatial variation in the age of metamorphism, the presence of mineral inclusions that influence the Sm/Nd ratio of the host phase, or Sm/Nd zoning resulting from long-term growth or polymetamorphism at temperatures too low to cause complete intracrystalline diffusion.

Ages obtained on Western Gneiss Region high-pressure rocks by U/Pb and U–Th/Pb dating have tended to be younger than the Sm/Nd ages. Gebauer et al.'s [11] U/Pb TIMS study of zircons from five eclogites from the Stadlandet region (Fig. 1) revealed a lower intercept age of 446 (+54/−65) Ma for one sample, whereas three other discordant zircon fractions had $^{238}U/^{206}Pb$ ages between 422 and 398 Ma. In situ ion microprobe analysis of monazite included within a garnet from microdiamond-bearing kyanite-garnet gneiss on the island of Fjørtoft (Fig. 1) yielded a 415±7 Ma age interpreted as predating UHP garnet growth based on garnet major element zoning [12]. U/Pb zircon dating of the Hareidland eclogite (Fig. 1) has been attempted twice. The initial study [13]

Table 1
Sm/Nd ages (2σ) of HP–UHP eclogites, Western Gneiss Region

Location	Isochron	Age (Ma)	MSWD	Ref.
Or, Frei	gar-cpx	407±17[a]		[29]
Gryttingvåg	gar-cpx	447±14[a]		[29]
Ulsteinvik	gar-cpx	422±19[a]		[29]
Raudberg	gar-cpx	423±8[a]		[29]
Tverrfjell	gar-cpx	418±27[a]		[29]
Almklovdalen	gar-cpx	408±6[a]		[5]
	gar-cpx-WR	407±76[a]	3.7[a]	
Eiksunddal	gar-cpx	412±4[a]		[6]
Flemsøya	gar-cpx-WR	410±16[a]	0.2[a]	[7]
Saltaneset	gar-cpx-WR	408.3±6.7	0.8	[8]

[a] Recalculated assuming Sm/Nd uncertainties of ±0.5%, using the Isoplot program of Ken Ludwig (rev. 2.49). "gar": garnet, "cpx": clinopyroxene, "WR": whole rock.

obtained an age of 401±20 Ma, whereas a more recent study [14] yielded a weighted mean $^{207}Pb/^{206}Pb$ age of 401.6±1.6 Ma (MSWD=0.48) from four concordant multigrain fractions. In contrast, single zircon $^{238}U/^{206}Pb$ ages from Krogh et al. [15] define two stages of concordant zircon growth at 415 and 410 Ma from an eclogite on Averøya (inset, Fig. 1); the younger age was also found for zircon at Flemsøya (Fig. 1). Schärer and Labrousse [16] analyzed rutile and omphacite from an UHP eclogite at Drage (Fig. 1), reporting an U/Pb isochron age of 389±2 Ma (MSWD=0.78).

3. Focus of current study

This wide spread in zircon, monazite and Sm/Nd ages prompted us to conduct detailed U/Pb geochronology of four Western Gneiss Region eclogites to try to resolve whether the spread is geological or analytical, and to clarify the timing of UHP-HP metamorphism. One of these eclogites is from the core of the UHP terrane, two are from the mixed HP/UHP zone and one is from a more peripheral, perhaps lower pressure area. We made three types of measurements: thermal ionization mass spectrometry (TIMS) of multigrain separates, multi-step chemical abrasion of annealed multigrain separates [17–19] and sensitive high-resolution ion-microprobe (SHRIMP) analysis of portions of single grains. TIMS of multigrain separates yields the greatest precision, but potentially poorest accuracy because of the mixing of different age components and Pb loss. The strength of the chemical abrasion method, with high-temperature annealing followed by multi-step dissolution using HF acid at progressively higher temperatures, lies in its ability to remove common Pb and zones of Pb loss in initial steps, then to sequentially sample zircon domains with differing solubility, composition and, potentially, history [17–19]. Simple multi-step dissolution of zircon without prior thermal annealing in some cases yields elemental and isotopic leaching effects that can result in anomalous $^{206}Pb/^{238}U$ and $^{207}Pb/^{206}Pb$ ages [20–23]. These leaching effects are related to radiation damage, which is effectively eliminated by the high-temperature thermal annealing of the chemical abrasion technique [17–19]. SHRIMP is the least precise, but has the advantage of superior spatial resolution such that age components within individual grains can be resolved.

4. Analytical techniques

Zircon was separated from pulverized whole rock samples using a combination of heavy liquids, a Frantz Isodynamic Separator and hand picking. For TIMS analysis, grains with inclusions and fractures were excluded by hand picking under alcohol.

Zircon for SHRIMP analysis was mounted in epoxy, polished, and imaged with cathodoluminescence (CL) to reveal textural details such as zoning and metamorphic overgrowths. SHRIMP primary beam current ranged from −8 to −10 nA. Analysis times were 2 s for $^{90}Zr_2^{16}O$, 7 s for ^{204}Pb, 7 s for background, 12 s for ^{206}Pb, 10 s for ^{207}Pb, 5 s for ^{208}Pb, 6 s for ^{238}U, 3 s for $^{232}Th^{16}O$ and 3 s for $^{238}U^{16}O$. Following initial standardization with SL13, standardization during runs was accomplished using AS57 (radiogenic Pb/U=0.1875) grains mounted with the unknowns. Data are plotted on concordia diagrams with no common Pb correction. Correction using measured ^{204}Pb, generally <5 ppb, would impart unbearably large uncertainties to resulting $^{207}Pb/^{206}Pb$ ages, while poor correlation between Th/U and radiogenic $^{208}Pb/^{206}Pb$ rules out accurate correction using measured ^{208}Pb. Because the discordance described below is dominated by mixing and not by common Pb, the former can reasonably be assessed with uncorrected data. Quoted $^{238}U/^{206}Pb$ spot ages are corrected with measured ^{207}Pb.

Zircon used for TIMS analysis was washed for 20 min at 80 °C in 3.1 N HCl and then in 8 N HNO_3 prior to dissolution. The single step dissolution and the residue dissolutions from the chemical abrasion fractions were done for 2.5 days at 245 °C in Savillex® PFA vials in Parr® hydrothermal vessels beakers with a mixture of 50% HF and 8 N HNO_3.

The chemical abrasion fractions from the Flatraket and Verpeneset eclogites were first annealed at 850 °C for 48 h, followed by additional hand picking to remove cracked and non-zircon grains revealed by the annealing. Chemical abrasion steps, ranging from 120 to 190 °C, lasted 24 h and were spiked prior to dissolution. Complete pickup of dissolved material was ensured with three successive treatments in 3.1 N HCl at 120 °C, typically for 24, 48 and 48 h. The solution was combined, dried down and redissolved in 3.1 N HCl prior to column chemistry.

The small grain size of the Verpeneset chemical abrasion fraction precluded excluding rutile, zoisite and kyanite impurities by hand picking. Instead, the bulk sample was annealed, then subjected to multiple treatments with 50% HF on a hot plate, a treatment expected to have little effect on the very low-U zircon in this sample. Remaining impurities were assumed to have completely dissolved in the A step, given visual inspection and their expected solubilities in HF relative to zircon.

Trace element analysis of chemical abrasion solutions was accomplished on a Finnigan MAT Element 2 Inductively Coupled Plasma Mass Spectrometer at UCSB. Following extraction of U and Pb for TIMS analysis, solutions were diluted to either 1:121 or 1:1331. Detection limit estimates were calculated as three times the standard deviation of the blanks. The following masses were measured: Zr (96), Hf (180), Th (232), Nb (93), Ta (181), Y (89), La (139), Ce (140), Pr (141), Nd (142), Sm (152), Eu (153), Gd (158), Tb (159), Dy (164), Ho (165), Er (166), Tm (169), Yb (172), Lu (175). Zr and Hf were measured in high resolution mode; all other masses were measured in low resolution mode. The standardization solution contained neither Nb nor Ta; these were calibrated using the response of ^{89}Y and ^{175}Lu and applying the relationship 2/mass per amu. Precision was estimated from triplicate analysis of the residue of the <80-μm fraction, and ranges from 2.2% to 11% for the REE. Oxide interferences are substantially smaller than precision; thus, no correction was made. For example, the $^{142}Ce^{16}O$ interference on ^{158}Gd is estimated at 0.5%, compared to a precision of 4%. Elemental concentrations in zircon were determined from normalization with respect to Zr. Chondrite normalization of REE was done using the values of Sun and McDonough [24].

5. Rocks investigated

5.1. Flatraket

One of the more spectacular eclogites described by Wain [2] and Wain et al. [25] is the coesite-bearing rock exposed at Flatraket (Fig. 1). The peak UHP phases include garnet, omphacite, phengite, kyanite, rutile, coesite and amphibole (magnesiokatophorite with lesser edenite and pargasite). The omphacite and phengite are partially replaced by retrograde symplectites of diopside/hornblende+plagioclase and biotite+plagioclase, respectively. Each thin section contains a few carbonate pods up to 2 mm in size that consist of breunnerite ($Mg_{0.9}Fe_{0.1}CO_3$) rimmed by dolomite, plus garnet, amphibole, rutile, zircon and rare talc. Thermobarometry based on the assemblage garnet+omphacite+phengite yielded a temperature of 700 °C and a pressure of 2.4 GPa [3], on the low-pressure side of the quartz-coesite equilibrium. This estimate must represent post-peak pressure conditions, given the presence of inclusions of relict coesite within garnet [2] and omphacite (this study).

Zircon grains identified with optical and electron microscopy range from 5 to 50 μm, and are present as subrounded inclusions within garnet, omphacite, breunnerite, dolomite and quartz, as well as in symplectites after phengite and omphacite. Evidence for zircon growth at high pressure is discussed in Section 7.3.

5.2. Verpeneset

The aluminous eclogite from Verpeneset is noteworthy because of its near complete lack of retrogression and abundance of silicate phases in apparent equilibrium—garnet, omphacite, kyanite, phengite, quartz, amphibole and zoisite. Bryhni and Griffin [26] describe bands of two texturally distinct rock

types in outcrop: coarse-grained, foliated and lineated eclogite (type 1) and finer grained, kyanite-poor, unfoliated eclogite (type 2). Float samples used in this study resemble both these types, but not the flaser-textured eclogite reported by Carswell and Cuthbert [27]. This locale was initially placed within the HP coesite-free domain [2]. This is contradicted by recent findings of inclusions of polycrystalline quartz, after coesite, within garnet from both type-1 eclogite (this study; Fig. 2) and flaser eclogite [27], as well as estimated metamorphic conditions of 700 °C and 2.5 GPa for the former [28]. For this study, zircon was extracted only from type-2 eclogite.

Griffin and Brueckner [29] obtained Rb/Sr isotopic ratios from whole rock and six separated phases from type-1 eclogite, and reported a phengite–zoisite–omphacite–whole-rock isochron of 398±1 Ma (no MSWD). However, recalculation of their data shows that no single isochron can fit four or more ratios even assuming a liberal uncertainty of ±2% for $^{87}Rb/^{86}Sr$, though it is possible to calculate a phengite–zoisite–whole-rock isochron of 397±8 Ma (MSWD=0.23) or a phengite–omphacite–kyanite isochron of 398±51 Ma (MSWD=2.2).

5.3. Otnheim

Shoreline outcrops at Otnheim lie in the UHP zone (Fig. 1) and are notable for the preservation of UHP minerals within quartzofeldspathic gneiss [25]. We sampled a foliated, garnet–quartz–omphacite–rutile eclogite with centimeter-scale seams of quartz, garnet, zoisite, epidote and omphacite. Minor secondary phases include amphibole and carbonate. Inclusions of polycrystalline quartz and relict coesite in garnet are abundant. Zircon has not been identified in thin section.

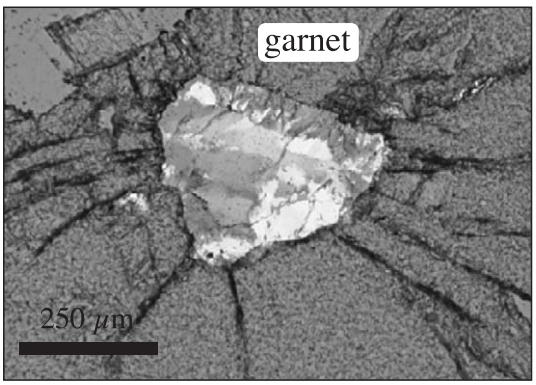

Fig. 2. Petrographic image of polycrystalline quartz pseudomorph after coesite, Verpeneset eclogite, demonstrating an UHP history for this sample; cross-polarized light, with 530-nm plate.

5.4. Langenes

We collected a previously unstudied Mg- and Ca-rich eclogite at Langenes on the island of Runde (Fig. 1). The eclogite contains garnet, sodic (Jd_{13}) diopside, magnesiohornblende and rutile, but no silica phase. An eclogite 2–3 km away contains relict coesite included within garnet [30], implying that the Langenes eclogite formed at ultrahigh pressure. Zircon was found only in mineral separates.

6. Geochronological results

6.1. Flatraket

Zircon grains from the Flatraket eclogite analyzed by SHRIMP range from 100 to 250 μm in size. Most grains show polygonal to fir-tree sector zoning or are unzoned in CL (Fig. 3a, left). Excluding three grains with demonstrable Pb loss, 28 $^{238}U/^{206}Pb$ spot ages range from 437 to 395 Ma (Fig. 4a), not defining a single population at the 95% confidence interval. One grain, #17, is distinguished by an interior domain with mottled CL (Fig. 3a, right); spot analyses throughout this grain yield the oldest (>421 Ma) $^{238}U/^{206}Pb$ ages, as well as generally lower U contents, higher Th/U ratios and more common Pb ($^{206}Pb_c$) (Table 2). Exclusion of analyses from grain 17 on the grounds of potential inheritance results in a range of $^{238}U/^{206}Pb$ ages from 420 to 395 Ma, but these ages still do not form a single population. The main cluster of analyses overlaps concordia at the 1σ level when uncorrected for common Pb (Fig. 4a) and all analyses are statistically concordant if corrected using measured ^{204}Pb (not shown). Implications of this range of apparently concordant analyses is discussed in Section 7.1.

In all, four multigrain fractions of zircon from the Flatraket eclogite were analyzed by TIMS, three of which were subjected to annealing and multi-step chemical abrasion (Table 3). The unannealed fraction

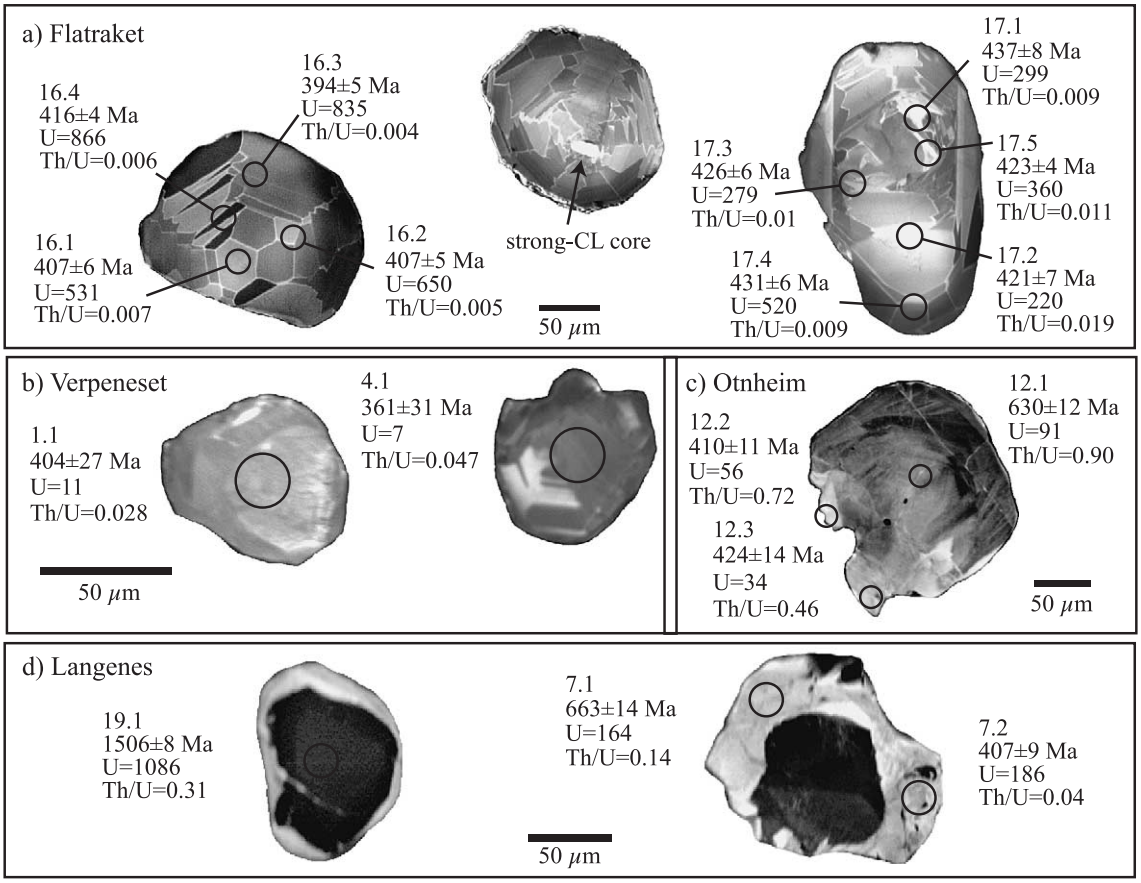

Fig. 3. Cathodoluminescence images of selected zircon grains analyzed by SHRIMP, with ^{207}Pb corrected ^{206}Pb/^{238}U ages (1σ) and U contents in ppm. (a) Well-developed sector zoning, with disturbed interior in grain 17 (right) and strong-CL core in unanalyzed grain (center). (b) Partial replacement of sector/oscillatory zoned region by faint, curved bands visible in grain 4. (c) Sparse, thin Caledonian rims surround inherited grains with faint oscillatory zoning. (d) Rims with lower U contents locally truncate faint zoning in higher U inherited cores; higher Th/U ratios and discordant spot ages from some rim analyses indicate solid-state recrystallization.

yielded a ^{238}U/^{206}Pb age of 404.4±0.8 Ma and a ^{207}Pb/^{206}Pb age of 411.8±1.0 Ma, equivalent to a weighted mean of the SHRIMP spot ages free of Pb loss. The three chemical abrasion fractions contained grain sizes of <80, 80–180 and 80–250 μm, and yielded six, seven and four abrasion steps, respectively, plus a final 'residue' step that dissolved all remaining zircon. Results from all three fractions are broadly similar, as shown on a ^{238}U release diagram (Fig. 5) and Tera-Wasserburg concordia plots (Fig. 4b,c). As the <80-μm fraction contained an order of magnitude more common Pb than the other fractions, and the A step of the 80–250-μm fraction did not contain measurable U and Pb, the details of the chemical abrasion will be discussed with respect to the 80–180-μm fraction.

The first two, A and B, dissolution steps removed <1% and ~3% of the total ^{238}U, respectively, as well as the majority of common Pb, resulting in poorly constrained ^{207}Pb/^{206}Pb ratios (Figs. 4b and 5). Thus, their young ^{238}U/^{206}Pb ages (379 and 400 Ma, respectively) could represent either late, minor growth of zircon or removal of soluble zones affected by Pb loss. The latter is a common feature in chemical abrasion analyses [19] and is supported by the three SHRIMP spot ages affected by Pb loss (Fig. 4a). The remaining steps are relatively free of common Pb (^{204}Pb/^{206}Pb≤0.000044) and yield well-constrained

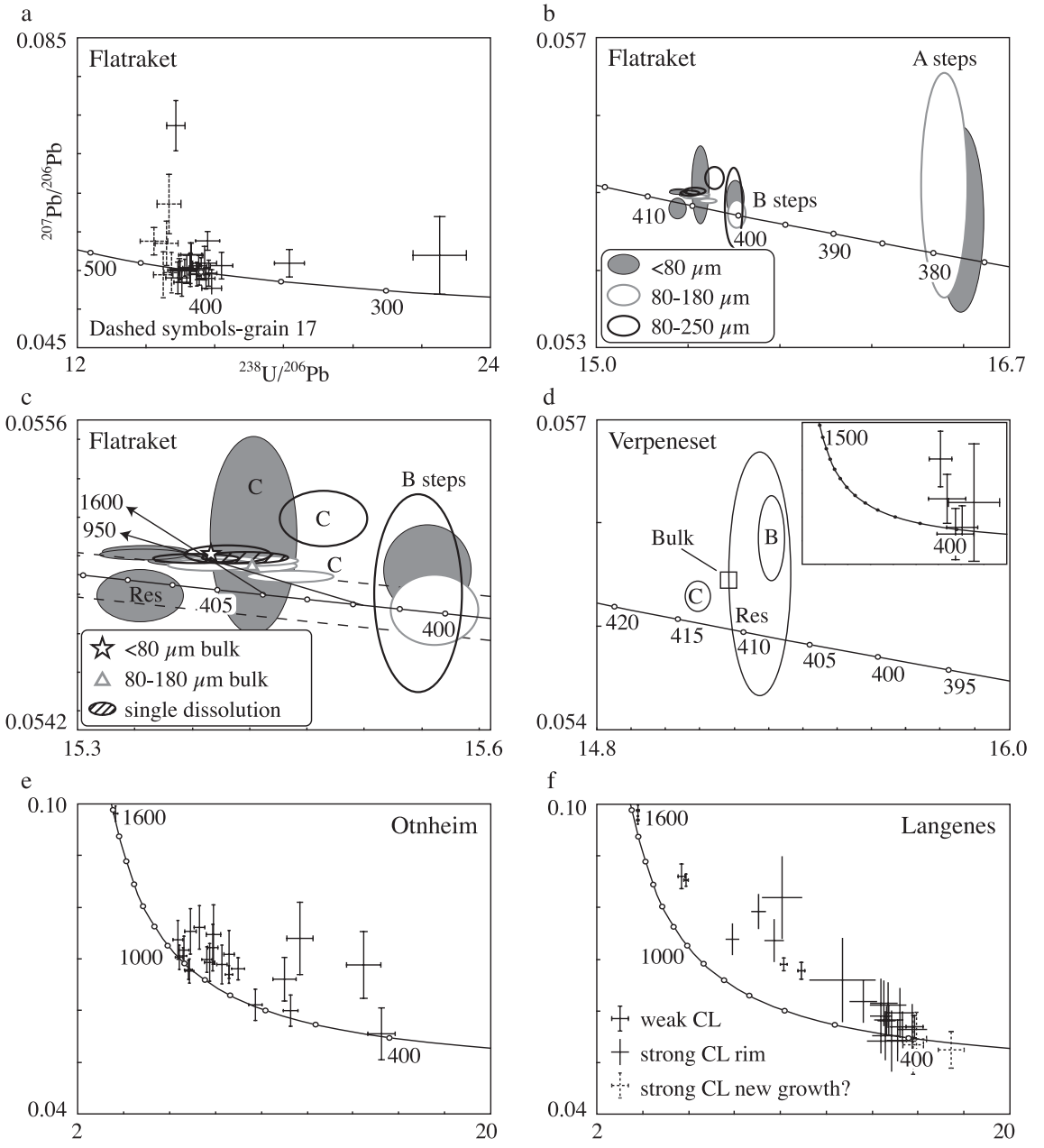

Fig. 4. Tera-Wasserburg concordia plots of SHRIMP and TIMS data. Concordia ages in Ma. All SHRIMP data plotted as 1σ crosses with no correction for common Pb (this correction has negligible effect on most analyses). All TIMS data except reintegrated bulk analyses plotted as 2σ ellipses. Lowest temperature chemical abrasion steps (A steps) from Flatraket eclogite show Pb loss. B steps indicate either minor growth at 400 Ma or remainder of Pb loss. Most steps are slightly discordant, even considering ±2σ decay constant uncertainties shown with dashed lines in (c).

$^{207}Pb/^{206}Pb$ ratios with 2σ age uncertainties of 0.8–1.0 Myr. Step C has a $^{207}Pb/^{206}Pb$ age that is 2 Myr younger than the remaining steps, which define a plateau with a $^{238}U/^{206}Pb$ age of 404.6±0.6 Ma (MSWD=1.2, n=5) and a $^{207}Pb/^{206}Pb$ age of 410.6±0.4 Ma (MSWD=1.3). The reintegrated bulk

Table 2
SHRIMP data (1σ)

Spot	U (ppm)	Th (ppm)	Th/U	Pb*[a] (ppm)	$^{206}Pb_c$[b] (%)	$^{238}U/^{206}Pb$	$^{207}Pb/^{206}Pb$	Conc. (%)	$^{206}Pb/^{238}U$ age[c] (Ma)	CL domain
Flatraket UHP eclogite (0302628, 6877367)										
17.1	299	3	0.0088	19	0.26	14.22 (27)	0.0587 (12)	79	437±8	interior
17.4	520	5	0.0087	33	0.13	14.50 (19)	0.0544 (20)	111	431±6	rim
17.3	279	3	0.0100	18	0.64	14.58 (22)	0.0584 (19)	78	426±6	rim
17.5	360	4	0.0115	22	0.02	14.74 (14)	0.0547 (17)	106	423±4	interior
17.2	220	4	0.0185	14	0.46	14.66 (23)	0.0635 (26)	59	421±7	rim
11.1	756	10	0.0126	46	0.08	14.92 (24)	0.0540 (13)	113	419±6	undiff[d]
1.1	433	4	0.0091	26	0.07	14.96 (22)	0.0550 (10)	101	417±6	undiff
4.1	766	5	0.0070	46	<0.01	14.99 (18)	0.05498 (78)	101	416±5	undiff
16.4	866	5	0.0063	52	<0.01	15.04 (15)	0.0534 (12)	119	416±4	undiff
12.1	914	3	0.0033	55	0.09	15.12 (10)	0.05534 (70)	97	413±3	undiff
15.3	694	3	0.0046	42	<0.01	15.18 (33)	0.0551 (12)	99	411±9	undiff
15.2	866	4	0.0041	57	2.59	14.86 (17)	0.0737 (22)	41	410±5	undiff
10.1	610	6	0.0093	36	0.05	15.28 (17)	0.0550 (14)	99	409±5	undiff
13.1	637	2	0.0029	38	0.02	15.28 (14)	0.0553 (13)	96	408±4	undiff
16.1	531	4	0.0071	32	0.27	15.30 (23)	0.0570 (11)	83	407±6	undiff
16.2	650	3	0.0045	39	0.15	15.32 (20)	0.0570 (10)	83	407±5	undiff
14.1	664	2	0.0032	39	0.03	15.47 (14)	0.05484 (72)	100	404±4	undiff
15.6	992	5	0.0054	58	0.07	15.47 (13)	0.0545 (10)	103	404±3	undiff
2.1	586	2	0.0029	34	0.05	15.53 (20)	0.05441 (92)	104	402±5	undiff
9.1	518	1	0.0023	30	0.05	15.53 (16)	0.05558 (87)	92	402±4	undiff
11.2	694	7	0.0097	40	<0.01	15.60 (17)	0.05522 (93)	95	400±4	undiff
6.1	692	4	0.0063	40	0.05	15.73 (17)	0.05395 (91)	108	398±4	undiff
3.1	408	<1	0.0008	24	0.18	15.70 (23)	0.0559 (14)	89	397±6	undiff
8.1	542	1	0.0025	31	0.02	15.82 (15)	0.0546 (11)	100	395±4	undiff
15.4	845	4	0.0043	48	0.09	15.91 (19)	0.0527 (16)	125	394±5	undiff
16.3	835	3	0.0036	48	0.12	15.79 (23)	0.05877 (82)	71	394±5	undiff
15.1	592	3	0.0045	33	0.08	16.19 (21)	0.0556 (11)	88	386±5	undiff
1.2	516	5	0.0095	26	0.02	18.16 (29)	0.0559 (12)	77	345±5	undiff
7.1	946	3	0.0027	38	0.02	22.52 (51)	0.0569 (33)	57	278±6	undiff
Verpeneset UHP eclogite (0300567, 6869159)										
5.1	10	<1	0.046	1	<0.01	14.20 (65)	0.0846 (78)	34	424±19	undiff
2.1	11	<1	0.030	1	1.06	14.8 (1.1)	0.0677 (68)	49	416±30	undiff
1.1	11	<1	0.028	1	1.42	15.5 (1.1)	0.0528 (72)	125	404±27	undiff
3.1	12	<1	0.036	1	<0.01	16.07 (91)	0.0557 (60)	89	389±21	undiff
4.1	7	<1	0.047	<1	0.02	17.1 (1.5)	0.066 (16)	45	361±31	undiff
Otnheim UHP eclogite (0311381, 6889619)										
4.1	1726	328	0.190	471	0.02	3.648 (58)	0.0981 (10)	98	1560±22	undiff
3.1	132	117	0.886	24	0.35	6.37 (14)	0.0737 (25)	91	937±19	undiff
5.1	111	162	1.456	23	0.37	6.43 (10)	0.0703 (16)	100	932±14	undiff
11.2	262	60	0.227	39	0.04	6.595 (94)	0.0706 (11)	96	909±12	undiff
5.2	95	96	1.006	17	0.62	6.63 (14)	0.0716 (18)	93	903±18	undiff
2.1	154	152	0.983	27	0.23	6.83 (11)	0.0679 (12)	102	882±13	undiff
2.2	102	86	0.848	17	0.07	6.87 (12)	0.0676 (15)	102	877±14	undiff
8.3	60	59	0.979	10	1.05	6.92 (18)	0.0753 (30)	81	863±21	undiff
1.1	38	17	0.449	6	1.01	7.30 (17)	0.0761 (28)	75	819±18	undiff
7.1	98	83	0.843	15	0.27	7.63 (14)	0.0698 (16)	86	790±14	undiff
8.1	122	132	1.087	19	0.05	7.75 (15)	0.0694 (24)	86	779±14	undiff

Table 2 (*continued*)

Spot	U (ppm)	Th (ppm)	Th/U	Pb*[a] (ppm)	$^{206}Pb_c$[b] (%)	$^{238}U/^{206}Pb$	$^{207}Pb/^{206}Pb$	Conc. (%)	$^{206}Pb/^{238}U$ age[c] (Ma)	CL domain
Otnheim UHP eclogite (0311381, 6889619)										
8.2	89	80	0.901	13	0.51	7.89 (15)	0.0723 (30)	77	762±14	undiff
1.2	52	27	0.518	7	0.63	7.93 (21)	0.0747 (39)	72	757±19	undiff
Otnheim UHP eclogite (0311381, 6889619)										
7.2	105	89	0.845	15	0.28	8.29 (14)	0.0690 (25)	82	730±12	undiff
10.2	215	389	1.813	36	0.31	8.596 (90)	0.0670 (12)	85	706±7	undiff
11.1	155	30	0.194	18	0.13	8.59 (13)	0.0709 (31)	74	703±11	undiff
10.3	166	255	1.539	25	<0.01	9.00 (18)	0.0681 (14)	78	675±13	undiff
7.3	88	72	0.817	11	0.02	9.34 (19)	0.0681 (18)	75	651±13	undiff
12.1	91	83	0.904	11	0.13	9.74 (19)	0.0611 (20)	98	630±12	undiff
6.1	58	35	0.612	6	1.54	11.01 (33)	0.0661 (28)	69	556±16	undiff
10.1	130	182	1.398	15	0.02	11.27 (20)	0.0600 (21)	91	547±10	undiff
6.2	67	51	0.760	7	0.36	11.70 (37)	0.0740 (47)	51	519±16	undiff
12.3	34	16	0.461	2	2.78	14.46 (50)	0.0688 (43)	48	424±14	rim
12.2	56	40	0.720	4	0.69	15.24 (40)	0.0555 (33)	94	410±11	rim
Langenes HP eclogite (0327346, 6923875)										
19.1	1086	339	0.312	294	0.02	3.788 (21)	0.09697 (52)	96	1506±8	weak CL
18.1	1072	261	0.243	284	0.03	3.805 (34)	0.09884 (66)	94	1496±12	weak CL
9.2	1812	480	0.265	319	0.02	5.695 (94)	0.0861 (16)	78	1029±16	weak CL
16.1	349	163	0.466	63	0.02	5.895 (51)	0.08532 (81)	76	996±8	weak CL
5.1	116	37	0.321	15	0.40	7.91 (17)	0.0739 (20)	74	760±16	strong CL rim
7.1	164	23	0.139	18	0.03	9.03 (20)	0.0793 (22)	57	663±14	strong CL rim
17.1	55	6	0.101	6	<0.01	9.73 (28)	0.0737 (27)	61	621±17	strong CL rim
1.1	432	115	0.266	42	0.05	10.15 (9)	0.06901 (86)	67	600±5	weak CL
2.2	109	26	0.238	11	0.38	10.08 (56)	0.0819 (53)	49	594±32	strong CL rim
15.1	532	336	0.631	54	0.36	10.91 (11)	0.0677 (11)	66	559±5	weak CL
11.1	14	2	0.137	1	1.05	12.72 (95)	0.0659 (53)	61	483±35	strong CL rim
11.2	66	4	0.0537	5	0.02	13.61 (39)	0.0618 (26)	69	454±13	strong CL rim
9.1	75	2	0.0313	5	0.15	14.37 (30)	0.0590 (47)	77	432±9	strong CL rim
10.1	94	9	0.0909	6	<0.01	14.56 (37)	0.0552 (31)	102	428±11	strong CL rim
6.2	58	1	0.0086	4	<0.01	14.51 (38)	0.0614 (29)	66	427±11	strong CL rim
3.2	129	4	0.0321	8	0.02	14.64 (24)	0.0580 (18)	80	425±7	strong CL rim
12.1	153	14	0.0943	10	0.09	14.73 (41)	0.0582 (18)	79	422±11	strong CL rim
6.1	66	<1	0.0044	4	0.02	14.70 (51)	0.0611 (28)	66	421±14	strong CL rim
4.1	48	2	0.0375	3	0.02	14.85 (68)	0.0541 (38)	112	421±19	strong CL rim
2.1	87	2	0.0232	5	0.57	15.10 (29)	0.0542 (26)	109	414±8	strong CL rim
13.1	83	4	0.0441	5	0.32	15.21 (40)	0.0596 (31)	70	408±11	strong CL rim
7.2	186	8	0.0404	11	0.31	15.31 (35)	0.0569 (19)	84	407±9	strong CL rim
5.2	70	1	0.0194	8	18.13	12.72 (26)	0.201 (11)	17	402±10	strong CL rim
8.3	82	2	0.0286	5	<0.01	15.78 (29)	0.0535 (38)	114	397±7	strong CL
14.1	79	1	0.0176	5	0.50	15.74 (41)	0.0564 (32)	85	396±10	strong CL rim
12.2	392	38	0.0964	23	0.46	15.84 (25)	0.0569 (14)	81	393±6	weak CL
8.1	110	2	0.0212	6	<0.01	15.94 (27)	0.0546 (35)	100	392±7	strong CL
8.2	123	3	0.0229	6	<0.01	17.45 (37)	0.0525 (23)	118	360±7	strong CL

[a] Radiogenic Pb.

[b] Common Pb component (%) of total ^{206}Pb, determined using measured ^{204}Pb.

[c] Corrected for common Pb using ^{207}Pb, assuming concordance other than common Pb.

[d] Undifferentiated.

Table 3
U/Pb TIMS data (2σ)

Fraction (μm)	CA step[a]	% ^{238}U	Conc (ppm)		Isotopic ratios (absolute error)				Ages (Ma)	
			U	Pb	^{204}Pb/^{206}Pb	^{208}Pb/^{206}Pb	^{238}U/^{206}Pb	^{207}Pb/^{206}Pb	^{238}U/^{206}Pb	^{207}Pb/^{206}Pb
Flatraket eclogite (0302628, 6877367)										
<80	A (120 °C)	0.86	341	19.6	0.002352	0.0932	16.585 (83)	0.0546 (10)	377 (2)	398 (41)
	B (160 °C)	5.84	371	21.8	0.000463	0.0201	15.605 (31)	0.05492 (19)	400.4 (8)	409.1 (7.8)
	C (170 °C)	23.90	408	24.8	0.001711	0.0680	15.453 (31)	0.05511 (42)	404.2 (8)	417 (17)
	D (170 °C)	25.22	410	24.2	0.000026	0.0045	15.400 (31)	0.054973 (21)	405.6 (8)	411.1 (9)
	E (180 °C)	17.85	379	22.5	0.000032	0.0048	15.357 (31)	0.055006 (23)	406.7 (8)	412.5 (9)
	F (180 °C)	22.77	381	22.6	0.000046	0.0051	15.359 (31)	0.055021 (26)	406.6 (8)	413.1 (1.1)
	Res (245 °C)	3.56	366	21.8	0.000191	0.0105	15.355 (31)	0.05479 (11)	406.7 (8)	403.8 (4.5)
	Bulk	100.00	393	23.4	0.000486	0.0218	15.416	0.05501	405	413
80–250[b]	B (160 °C)	2.96	403	23.9	0.001003	0.0411	15.597 (31)	0.05480 (42)	400.6 (8)	404 (17)
	C (170 °C)	5.84	431	25.3	0.000137	0.0080	15.514 (31)	0.05519 (12)	402.7 (8)	420.0 (4.7)
	D (180 °C)	10.99	448	26.4	0.000036	0.0046	15.431 (31)	0.055006 (37)	404.8 (8)	412.5 (1.5)
	Res (245 °C)	80.21	465	27.4	0.000010	0.0035	15.403 (31)	0.054987 (19)	405.5 (8)	411.7 (8)
	Bulk	100.00	459	27.1	0.000050	0.0050	15.418	0.05500	405	412
80–180	A (120 °C)	0.51	365	21.2	0.002805	0.1092	16.514 (83)	0.0551 (12)	379 (2)	416 (49)
	B (160 °C)	3.01	371	21.7	0.000330	0.0145	15.611 (31)	0.05472 (15)	400.3 (8)	400.8 (6.1)
	C (170 °C)	11.38	403	23.7	0.000038	0.0036	15.485 (31)	0.054893 (24)	403.4 (8)	407.9 (1.0)
	D (170 °C)	13.06	408	24.0	0.000035	0.0036	15.455 (31)	0.054975 (23)	404.2 (8)	411.2 (9)
	E (180 °C)	10.91	405	23.8	0.000044	0.0040	15.453 (31)	0.054947 (26)	404.2 (8)	410.1 (1.0)
	F (180 °C)	24.55	402	23.7	0.000021	0.0032	15.445 (31)	0.054950 (20)	404.4 (8)	410.2 (8)
	G (190 °C)	23.34	387	22.8	0.000037	0.0040	15.416 (31)	0.054952 (23)	405.2 (8)	410.3 (1.0)
	Res (245 °C)	13.25	385	22.7	0.000031	0.0037	15.425 (31)	0.054973 (22)	404.9 (8)	411.1 (9)
	Bulk	100.00	396	23.3	0.000056	0.0045	15.453	0.05494	404	410
80–160[c]			412	24.2	0.000040	0.0055	15.446 (31)	0.054990 (24)	404.4 (8)	411.8 (1.0)
Verpeneset eclogite (0300567, 6869159)										
10–50[b]	B (160 °C)	34.81	14.0	0.84	0.000571	0.0981	15.306 (31)	0.05588 (33)	408.0 (8)	447 (13)
	C (170 °C)	57.07	20.2	1.22	0.000222	0.1435	15.095 (30)	0.05529 (12)	413.5 (8)	424.1 (4.8)
	Res (245 °C)	8.12	23.3	1.47	0.003155	0.2379	15.273 (76)	0.0555 (10)	409 (2)	434 (39)
	Bulk	100.00	18.3	1.11	0.000582	0.1354	15.183	0.05552	411	433

[a] Chemical abrasion steps, with temperature; bulk reintegrated isotopic ratios weighted with respect to % ^{238}U released.
[b] The A step contained negligible U, Pb and was not analyzed.
[c] Unannealed, single dissolution fraction.

analysis of this fraction, weighted with respect to % ^{238}U released in individual steps, has a ^{238}U/^{206}Pb age of ~404 Ma and a ^{207}Pb/^{206}Pb age of ~410 Ma.

The slightly older ^{207}Pb/^{206}Pb ages of the higher temperature chemical abrasion steps might reflect mixing between a minor inherited component and a dominant metamorphic component, or they might be due to a combination of factors unrelated to inheritance of older zircon, such as decay constant errors and intermediate daughter product disequilibrium effects. These potential causes of apparent discordance and our reasons for favoring the inheritance interpretation are discussed in detail in Section 7.2.

6.2. Verpeneset

Zircon grains from the Verpeneset eclogite selected for SHRIMP are 40–60 μm and, in CL, show regions of variably defined oscillatory zoning that are partially replaced by crystal with faint, curved zoning (Fig. 3b), implying incomplete solid-state recrystallization [31]. Because of extremely low U contents (~10 ppm), we analyzed only five grains by SHRIMP. Two analyses are normally discordant; however, the ^{204}Pb abundances are too low to yield a reliable correction, thus all analyses are shown uncorrected (Fig. 4d, inset). If a single concordant episode of zircon growth is

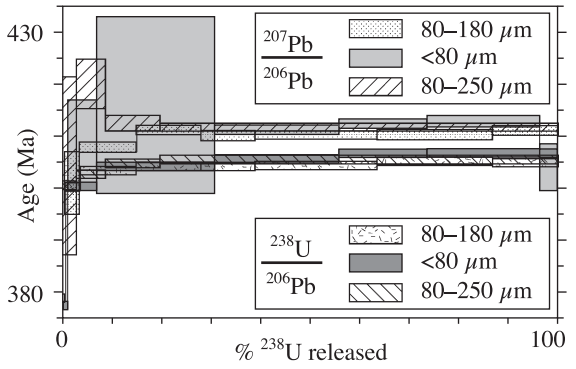

Fig. 5. Flatraket eclogite chemical abrasion step ages (2σ) vs. cumulative ^{238}U released. The lowest temperature ("A") steps from two size fractions yield lower ^{206}Pb/^{238}U ages (A step ^{207}Pb/^{206}Pb ages not shown, as 2σ uncertainties are off scale). The A step of the 80–250-μm fraction contained negligible U, Pb and was not analyzed. Remaining steps show slight discordance. Ages from the <80-μm fraction are 1–2 Myr older than those from the 80–180-μm fraction.

assumed, a ^{207}Pb correction for common Pb can be applied, yielding a weighted mean ^{238}U/^{206}Pb age of 403±21 Ma (MSWD=0.92).

A 10–50-μm chemical abrasion fraction yielded three dissolution steps plus a residue (Fig. 4d, Table 3). The A step contained negligible U and Pb and was not analyzed. The B step extracted 35% of the total ^{238}U, and yielded ^{238}U/^{206}Pb and ^{207}Pb/^{206}Pb ages of 408.0±0.8 and 447±13 Ma, respectively. The C step extracted 57% of the total ^{238}U, with ^{238}U/^{206}Pb and ^{207}Pb/^{206}Pb ages of 413.5±0.8 and 424±5 Ma, respectively. Little material remained for the residue step, which yield ^{238}U/^{206}Pb and ^{207}Pb/^{206}Pb ages of 409±2 and 434±39 Ma, respectively. The bulk reintegrated sample has ^{238}U/^{206}Pb and ^{207}Pb/^{206}Pb ages of 411 and 433 Ma, respectively. The B and C steps, as well as the bulk sample, are clearly discordant (Fig. 4d).

6.3. Otnheim

Zircons separated from the Otnheim eclogite are 50–250-μm subequant grains and grain fragments. CL imaging and SHRIMP demonstrate that the zircons are composed predominantly of inherited material with variably developed oscillatory zoning and high Th/U ratios (mean ~1.0) (Fig. 3c, Table 2). Most SHRIMP analyses reveal 60–260 ppm U and yield an array of ^{206}Pb/^{238}U ages between ~700 and ~950 Ma; one concordant spot age is ~1.6 Ga (Fig. 4e). Two analyses from thin, low U (<60 ppm) rims yielded ^{207}Pb-corrected ^{206}Pb/^{238}U ages of 410±11 and 424±14 Ma. Intermediate spot ages may represent mixing of ~950 and ~400 Ma components.

6.4. Langenes

Zircon occurs as 50–150-μm rounded to elongate grains with high U (mean ~500 ppm) cores and low U (50–200 ppm) rims in the Langenes eclogite (Fig. 3d). Grain cores show either no zoning or faint sector zoning; where present, core zoning is truncated by rims and along fractures with stronger CL response and patchy zoning and locally developed arcuate banding. While these textural relationships are inconclusive, some rim ages lie between the main cluster at ~400 Ma and protolith age(s) (Fig. 4f), indicating rim formation by incomplete recrystallization of inherited zircon rather than new overgrowth on detrital cores [31]. One grain shows only strong CL response and may indicate late growth or Pb loss (Fig. 4f). Excluding analyses from this grain, all 25 SHRIMP spot ages are consistent with mixing among 1.6 Ga, 400 Ma and possibly 950 Ma components. The potential presence of more than two components precludes determination of the Caledonian lower intercept.

7. Interpretation

7.1. SHRIMP/CL results, Flatraket eclogite

The most useful data from this study for assessing the age of UHP metamorphism in the WGR are derived from the Flatraket eclogite. A simple, single-age zircon population for this sample is precluded by the ~40 Myr spread in SHRIMP ^{206}Pb/^{238}U ages, leaving two possible end-member scenarios: (i) ~400 Ma crystallization of zircon with minor discordance due to inheritance or (ii) new growth of concordant zircon from ~437 to ~395 Ma. However, uncertainties in SHRIMP ^{207}Pb/^{206}Pb ratios for zircons of this age and U content are substantial enough to conceal the minor discordance expected from ~400 Ma zircon with a minor

inherited 1600–950 Ma component (Fig. 4c), the latter range including likely protolith ages from eclogites nearby Flatraket [11], and the oldest SHRIMP spot ages from Otnheim and Langenes (Fig. 4e,f). Thus, the fact that one grain (#17) yielded the five oldest $^{206}Pb/^{238}U$ spot ages is equivocal. This grain may contain the greatest inherited component of those analyzed by SHRIMP, potentially indicated by its different Th and U contents (Fig. 3a). Alternatively, it could represent the earliest phase of zircon crystallization in conditions resulting in different zircon chemistry.

7.2. Discordant Flatraket TIMS data and linear regression

Potential causes of discordance in metamorphic zircon include Pb loss, inheritance and secular disequilibrium of intermediate daughter products during crystallization or metamorphism. Additionally, inaccuracy in accepted decay constants can cause slight apparent discordance. Accurate age determination from the Flatraket TIMS data hinges on proper interpretation of the observed discordance in the high-temperature (C and later) chemical abrasion steps. These steps extracted more than 95% of the zircon, yielding a narrow, 407–403 Ma, range in $^{206}Pb/^{238}U$ ages (Fig. 5). All but three of these steps have well-constrained $^{207}Pb/^{206}Pb$ ages (2-σ errors <2 Myr), and are slightly but distinctly discordant, even when uncertainties in the accepted decay constants of Jaffey et al. [32] are considered (Fig. 4c). Discordance of these steps due to Pb loss is improbable given how efficiently low-temperature abrasion steps remove domains of Pb loss [19].

Apparent discordance in other studies has been attributed to secular disequilibrium of intermediate daughter products, such as exclusion of ^{230}Th or enrichment or ^{231}Pa during crystallization, and loss of ^{222}Rn during prolonged high-temperature metamorphism. But, the complete exclusion of ^{230}Th during crystallization of ~400 Ma zircon will likely yield <1 Myr discordance, less than that discussed here. Anomalous 20–40% discordance of baddeleyite from Île Bizard has been attributed to loss of ^{222}Rn during prolonged high-temperature metamorphism [33]. Hypothetically, loss of, for example, 20% of Rn over 4 Myr would raise apparent $^{207}Pb/^{206}Pb$ ages by ~5 Myr, enough to explain the observed discordance, but such behavior has not been identified in zircon. Another potential source of anomalous discordance in zircon is the incorporation of ^{231}Pa in excess of secular equilibrium. Anczkiewicz et al. [34] attributed this effect to discordance, far greater in magnitude than observed in the present study, in low-Th/U zircon from an alkali-granite dike in the Himalaya. Although it is impossible to rule out either Rn loss or incorporation of excess ^{231}Pa as the cause of artificially high $^{207}Pb/^{206}Pb$ ages, neither can account for the spread in $^{206}Pb/^{238}U$ ages from the Flatraket eclogite.

For these reasons, we favor an interpretation of discordance due to minor inheritance of pre-Caledonian zircon, with additional evidence arising from the observation of strong-CL cores in multiple zircon grains selected for inclusion analysis (Fig. 3a, center). Cores are estimated to comprise ≤1% of zircon in this grain mount, comparable with the extent of discordance observed in the high-temperature chemical abrasion steps assuming a protolith age between 1.6 Ga and 950 Ma. Unfortunately, no age determinations have been made on these cores.

Linear regression of the high-temperature Flatraket abrasion steps by themselves is fruitless, due to the very narrow spread of isotopic ratios. A more appropriate treatment involves fixing the upper intercept to the extremes of likely protolith ages, 1.6 Ga and 950 Ma, and calculating a range of possible lower intercept ages. The A and B steps, likely affected by Pb loss, are excluded, as is the 80–250-μm C step, which likely suffered from discrimination effects (Fig. 5). The resulting range of lower intercept ages, 405–400 Ma, is considered the best estimate for zircon crystallization in the Flatraket eclogite.

While these systematics of U/Pb behavior are best documented for the Flatraket eclogite, the Verpeneset, Otnheim and Langenes eclogite zircons yield U/Pb ages and CL textures that are consonant with this interpretation, implying that all were metamorphosed at ~400 Ma. The response to metamorphism varies between samples: partial recrystallization of pre-Caledonian igneous zircon in the Langenes and Verpeneset eclogites, and crystallization of zircon as new grains and overgrowths on inherited cores in the Flatraket and Otnheim eclogites.

Table 4
Zircon trace element data

	Flatraket eclogite fractions																								Verpeneset eclogite				
	<80 (μm)								80–250 (μm)						80–180 (μm)										80–160 (μm)	10–50 (μm)[a]			
CA step	A	B	C	D	E	F	Res	Bulk[b]	A	B	C	D	Res	Bulk[b]	A	B	C	D	E	F	G	Res	Bulk[b]		B	C	Res	Bulk[b]
Temp. (°C)	120	160	170	170	180	180	245		120	160	170	180	245		120	160	170	170	180	180	190	245			160	170	245	
% sample[b]	0.99	6.18	23.00	24.15	18.46	23.42	3.81	100	0.64	3.34	6.19	11.18	78.66	100	0.56	3.21	11.18	12.67	10.67	24.20	23.89	13.62	100	100	43.93	49.91	6.15	100
Hf[c]	1.39	1.60	1.58	1.56	1.59	1.56	1.50	1.57	1.45	1.49	1.55	1.56	1.55	1.55	1.62	1.59	1.64	1.90	1.59	1.74	1.72	1.61	1.71	1.68	1.51	1.48	1.49	1.49
Y	195	21	25	26	29	29	31	28	257	27	26	25	24	26	183	22	22	22	25	26	27	29	26	28	45	71	71	60
Nb[d]	7.4	1.6	1.8	1.4	2.1	1.7	2.7	1.8	17.9	2.4	1.6	1.4	1.1	1.3	5.3	1.4	1.3	1.2	1.4	1.6	1.1	1.5	1.4	1.2	1.2	1.6	2.8	1.5
Ta[e]	1.4	0.31	0.46	0.23	0.47	0.38	0.37	0.39	1.7	0.43	0.22	0.52	0.17	0.23	0.68	0.18	0.19	0.29	0.25	0.34	0.14	0.16	0.23	0.35	0.14	0.36	0.93	0.30
Th	37	3.7	5.2	7.1	6.2	5.8	4.8	6.2	31	4.9	4.4	6.7	3.7	4.3	24	2.2	2.9	3.5	3.4	4.1	3.4	3.4	3.6	5.8	3.7	9.6	8.6	7.0
U	341	371	408	410	379	381	366	392	N/A	403	431	448	465	456	365	371	403	408	405	402	387	385	396	412	14	20	23	18
Pb	19.6	21.8	24.8	24.2	22.5	22.6	21.8	23.3	N/A	23.9	25.3	26.4	27.4	26.9	21.2	21.7	23.7	24.0	23.8	23.7	22.8	22.7	23.3	24.2	0.8	1.2	1.5	1.1
La	1.10	0.09	0.09	0.31	0.15	0.05	0.42	0.17	2.96	0.21	0.11	0.03	0.02	0.05	1.88	0.04	0.15	0.07	0.16	<	<	0.09	<	0.06	0.04	0.09	0.05	0.07
Ce	25.8	1.31	1.50	1.80	1.62	1.40	2.06	1.82	31.0	1.60	1.38	1.27	1.19	1.41	25.7	1.31	1.54	1.44	1.76	1.63	1.48	1.54	1.69	1.19	0.27	0.46	0.35	0.37
Pr	2.97	0.08	0.04	0.11	0.08	0.04	0.16	0.10	4.90	0.14	0.07	0.04	0.01	0.06	2.88	0.08	0.02	0.02	0.06	0.02	<	0.02	<	0.03	0.03	0.05	0.07	0.04
Nd	29.0	0.63	0.61	0.87	0.64	0.53	1.14	0.96	39.9	1.06	0.60	0.48	0.48	0.76	28.0	0.64	0.74	0.72	0.72	0.51	0.37	0.51	0.71	0.55	0.29	0.26	0.33	0.28
Sm	38	<	<	<	<	<	<	<	53	<	<	<	0.46	<	41	<	<	<	<	<	<	<	<	<	<	<	<	<
Eu	10.0	0.31	0.30	0.37	0.42	0.46	0.47	0.48	13.9	0.38	0.32	0.30	0.33	0.41	9.26	0.37	0.39	0.41	0.43	0.47	0.41	0.50	0.48	0.40	0.19	0.30	0.31	0.25
Gd	50.3	2.1	2.6	2.6	2.8	3.3	3.5	3.3	67.2	2.5	2.3	2.2	2.3	2.7	45.8	2.3	2.7	2.4	3.0	3.2	3.1	3.3	3.2	2.7	1.1	1.7	1.7	1.4
Tb	5.57	0.42	0.47	0.58	0.61	0.58	0.72	0.61	7.54	0.58	0.53	0.51	0.47	0.52	4.90	0.43	0.44	0.49	0.54	0.58	0.71	0.67	0.61	0.53	0.50	0.71	0.74	0.62
Dy	33.1	2.7	3.7	3.9	4.1	4.4	4.6	4.2	41.4	3.6	3.7	3.4	3.4	3.6	31.5	3.2	3.3	3.5	3.8	4.1	4.3	4.3	4.1	3.8	5.8	8.3	8.6	7.2
Ho	7.01	0.73	0.88	0.83	0.90	0.93	1.02	0.94	8.73	0.86	0.85	0.85	0.74	0.81	6.38	0.75	0.76	0.72	0.79	0.86	0.94	0.96	0.89	0.94	1.49	2.40	2.39	2.00
Er	21.2	2.5	2.9	3.0	3.2	3.0	3.2	3.2	28.9	3.6	3.4	3.0	2.6	2.9	21.7	2.7	2.4	2.4	2.5	2.6	2.7	2.9	2.7	3.4	5.6	10.5	10.6	8.4
Tm	3.15	0.42	0.59	0.51	0.50	0.60	0.62	0.57	4.11	0.47	0.56	0.48	0.42	0.46	3.72	0.41	0.50	0.50	0.64	0.48	0.43	0.44	0.50	0.54	1.15	2.41	2.20	1.84
Yb	23.9	3.5	4.2	4.3	4.7	4.6	4.1	4.6	30.4	4.6	4.4	4.1	3.0	3.4	23.7	3.4	2.9	3.0	3.1	2.9	3.1	3.1	3.2	4.4	10.0	22.1	21.6	16.8
Lu	4.21	0.70	0.90	0.93	0.96	1.04	0.87	0.97	5.36	0.86	0.84	0.76	0.58	0.65	4.24	0.66	0.54	0.55	0.57	0.54	0.49	0.55	0.56	0.90	2.25	5.15	4.87	3.86

(<) Below detection limit.

[a] Verpeneset A step not analyzed.

[b] Normalized with respect to Zr.

[c] Wt.%; all other data in μg/g.

[d] Based on response of Y^{89} with 8.6% mass bias correction (2/mass per amu).

[e] Based on response of Lu^{175} with 6.6% mass bias correction (2/mass per amu).

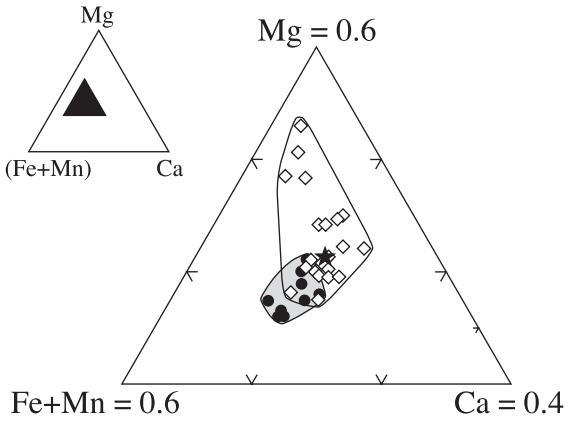

Fig. 6. Compositions of garnet from inclusions within zircon (filled circles) and matrix (open diamonds), Flatraket eclogite. Average matrix composition shown by star.

7.3. Metamorphic conditions

High precision U/Pb zircon ages from metamorphic rocks are most useful if they can be related to *P–T* conditions derived from major phases. For the Flatraket eclogite, two lines of evidence—types and compositions of inclusions within zircon, and zircon REE patterns—indicate that zircon crystallization occurred at, or shortly after the peak of HP metamorphism. Inclusions in Flatraket zircons consist mainly of garnet with minor rutile, omphacite and pargasite, demonstrating eclogite-facies zircon crystallization. Compositions of garnet inclusion are similar to, but slightly richer in almandine than those of homogenized matrix porphyroblasts, suggesting zircon crystallization at slightly sub-peak temperature (Fig. 6).

To further assess conditions of zircon crystallization, solutions remaining after removal of U and Pb for TIMS were analyzed for trace element abundances with ICP-MS. Measurements near detection limit resulted in increased variability in the LREE, particularly La and Pr. Concentrations of Sm in all but the A steps and the 80–250-μm fraction residue were below the particularly high detection limits for this element. As concentrations in zircon were determined by normalization with respect to Zr, and no correction

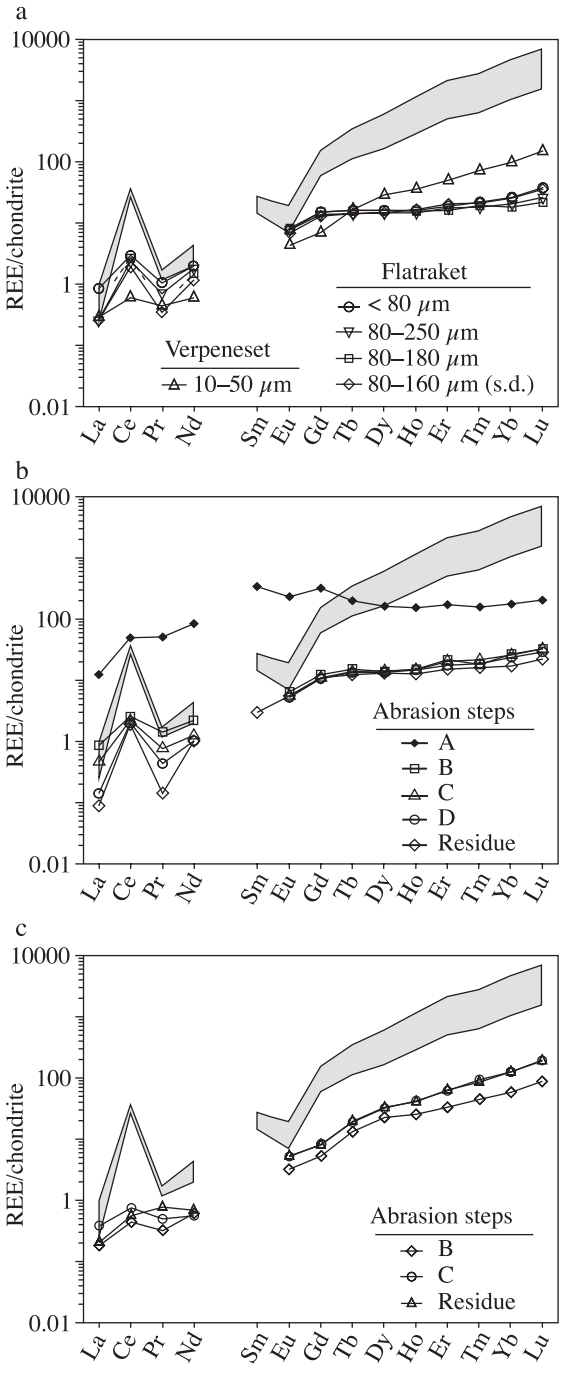

Fig. 7. Chondrite-normalized REE profiles from chemical abrasion solutions. (a) Reintegrated bulk analyses for all chemical abrasion fractions, with Flatraket single dissolution fraction. (b) Flatraket eclogite: 80–250-μm fraction; results from other size fractions are similar. Aside from a distinctly enriched A step, all steps yield shallow HREE and negligible Eu anomaly. (c) Verpeneset eclogite: 10–50-μm chemical abrasion fraction. Intermediate HREE slopes may arise from mixture of Caledonian eclogite-facies and inherited pre-Caledonian igneous zircon. Shaded field: typical igneous zircon profile; aplite from the Boggy Plain zoned pluton [35].

was made for Hf, the concentrations shown in Table 4 are overestimated by 1–2%. However, only relative abundances are considered in the following discussion.

Flatraket zircon REE concentrations for the three recombined bulk abrasion fractions and the single dissolution fraction are nearly identical (Fig. 7a) Other than the distinct A steps discussed in the following paragraph, consistency of concentrations of individual steps of each chemical abrasion fraction is observed, as exemplified by the 80–250 μm fraction (Fig. 7b). Because REE decrease with increasing mass, the HREE preferentially substitute for smaller Zr^{4+} cations in the zircon lattice; thus, igneous and most metamorphic zircon exhibit steep slopes, exemplified by aplite from the Boggy Plain zoned pluton (Fig. 7) [35]. However, zircon that crystallized during or after substantial growth of garnet, which also sequesters HREE much more than LREE, exhibit much shallower, sometimes negative, HREE slopes [36–40]. The flat HREE profiles from the Flatraket eclogite (Fig. 7a,b) zircon demonstrate crystallization in the presence of, or after considerable growth of pyrope-rich, eclogite-facies garnet.

While REE valences are typically 3+, Ce can also occur as a 4+ cation and Eu can occur as a 2+ cation. The former can substitute directly for Zr^{4+} in zircon, causing the positive Ce anomaly commonly observed in zircon [36]. Plagioclase preferentially incorporates Eu^{2+}, leading to both positive and negative bulk-rock Eu anomalies, while growth of zircon in the presence of plagioclase yields negative Eu anomalies in zircon [37]. Assessment of Eu anomalies in the present dataset is hindered by particularly high detection limits for Sm, the element adjacent to Eu. The 80–250-μm residue from the Flatraket eclogite, however, has no Eu anomaly (Fig. 7b), suggesting zircon crystallization in the absence of plagioclase [37,40]. Thus, REE data indicate zircon from the Flatraket eclogite crystallized in the eclogite facies, specifically in the presence of pyrope-rich garnet and in the absence of plagioclase.

Trace element concentrations in the A steps from all three Flatraket chemical abrasion fractions are 5–50 higher than those in the remaining steps, except for Hf, U and Pb, which are equivalent or slightly lower (Table 4). Additionally, the A steps are noticeably enriched in LREE compared to later steps (Fig. 7b). The small volume of zircon in these steps was likely sampled from μm-scale rims rich in trace elements, and thus more soluble than remaining zircon. The younger, ~380 Ma, $^{206}Pb/^{238}U$ ages from the two analyzed A steps are consistent with either minor Pb loss or late growth of thin rims (Fig. 4b). The former is considered more likely, given the Pb loss observed in some SHRIMP analyses (Fig. 4a).

The Verpeneset eclogite chemical abrasion solutions, both those from individual steps and the recombined bulk analysis, yielded HREE slopes intermediate between those from Flatraket and Boggy Plain zoned pluton aplite [35] (Fig. 7a,c). This most likely represents a mixture of Caledonian eclogite-facies zircon and inherited, pre-Caledonian, igneous zircon with steep HREE and oscillatory zoning (Figs. 3b and 4d). All Sm measurements from this sample were below detection limit, preventing accurate assessment of Eu anomalies.

7.4. Comparison with existing geochronology

Our preferred age of 405–400 Ma for the Flatraket eclogite agrees with the 401.6±1.6 Ma age from the Hareidland eclogite [14]. Coesite inclusions within Hareidland zircon demonstrate some component of growth at UHP conditions [14]; it is possible that these zircons grew in more than one stage, but there are no CL images to assess this possibility.

The youngest of all U/Pb eclogite ages reported is the rutile-omphacite age of 389±2 Ma from Drage (Fig. 1), interpreted to represent rutile closure at 770 °C and 1.8 GPa, the peak temperature experienced by this sample [16]. However, this temperature lies above closure temperatures for Pb in rutile determined from experiments (600 °C [41]) and from field-based studies (400–450 °C [42]), and all rutiles from WGR eclogites that we have examined contain plates of ilmenite that probably exsolved after the UHP event. Thus, the 389 Ma age more likely corresponds to a later stage of exhumation.

The 405–400 Ma Flatraket age is considerably younger than the 425 Ma mean age of Griffin and Brueckner [4] but it is equivalent to the more reliable three-point Sm/Nd isochron ages of 410±16 Ma from Flemsøya [7] and 408.3±6.7 Ma from Saltaneset [8], and slightly younger than the prograde 415±7 Ma monazite age from Fjørtoft [12]. Thus, within the limitations of the present dataset, all these eclogites formed in the 410–400 Ma interval, while slightly older

ages at Averøya [15], some 50 km to the NE, potentially indicate a larger scale age gradient within WGR eclogites.

7.5. Cooling and exhumation rates

The zircon crystallization in the Flatraket eclogite reported here occurred in the presence of garnet and in the absence of plagioclase, thus at any depth between ~100 and ~40 km. Subsequently, the UHP rocks were exhumed through the mantle and much of the crust prior to closure of K-white mica to Ar loss [43]. The Flatraket eclogite lies <10 km north of a K-white mica $^{40}Ar/^{39}Ar$ age of 389±4 Ma [1], implying cooling from ~750 to ~350 °C over a period of ~10–15 Myr, at a rate of ~20–30 °C/Myr. Exhumation from garnet-stable depths to ~15 km thus occurred at rates of >2.5–8.5 km/Myr.

8. Conclusions

Our TIMS, chemical abrasion and SHRIMP U/Pb zircon ages place significant new constraints on the history of Western Gneiss Region UHP-HP eclogites. Zircon from the Flatraket eclogite yields slightly discordant ages, representing crystallization at ~405–400 Ma with discordance from a minor component of inherited cores. Inclusion assemblages, CL imagery and trace element analysis (HREE profiles and Eu anomalies) indicate eclogite-facies, possibly post-peak conditions of crystallization. Greater components of inherited zircon in three other samples prevent precise determination of lower intercept ages, yet all yield results consistent with ~400 Ma metamorphism, adding to the growing body of evidence that the UHP-HP metamorphism is both substantially younger than the oft-quoted 425 Ma age, and coeval throughout the portion of the Western Gneiss Region shown in Fig. 1. In conjunction with $^{40}Ar/^{39}Ar$ K-white mica ages, our results indicate an exhumation rate of >2.5–8.5 km/Myr.

Acknowledgements

Funding sources for this project include NSF grant EAR-9814889, Sigma Xi, the American Federation of Mineralogical Societies and the Department of Geological Sciences at UCSB. In addition, the aid of Elizabeth Eide (Norwegian Geological Survey) and Torgeir Andersen (University of Oslo) is greatly appreciated. Georges Paradis provided invaluable assistance with acquisition and processing of ICPMS data. Finally, many thanks are due to Hannes Brueckner and Fernando Corfu for their insightful reviews of the manuscript.

References

[1] T.B. Andersen, Extensional tectonics in the Caledonides of southern Norway, an overview, Tectonophysics 285 (1998) 333–351.
[2] A. Wain, New evidence for coesite in eclogite and gneisses: defining an ultrahigh-pressure province in the Western Gneiss region of Norway, Geology 25 (1997) 927–930.
[3] S.J. Cuthbert, D.A. Carswell, E.J. Krogh-Ravna, A. Wain, Eclogites and eclogites in the Western Gneiss Region, Norwegian Caledonides, Lithos 52 (2000) 165–195.
[4] W.L. Griffin, H.K. Brueckner, Caledonian Sm–Nd ages and a crustal origin for Norwegian eclogites, Nature 285 (1980) 319–321.
[5] E.W. Mearns, Sm–Nd ages for Norwegian garnet peridotite, Lithos 19 (1986) 269–278.
[6] B. Jamtveit, D.A. Carswell, E.W. Mearns, Chronology of the high-pressure metamorphism of Norwegian garnet peridotites/pyroxenites, J. Metamorph. Geol. 9 (1991) 125–139.
[7] M.B.E. Mørk, E.W. Mearns, Sm–Nd isotopic systematics of a gabbro-eclogite transition, Lithos 19 (1986) 255–267.
[8] D.A. Carswell, H.K. Brueckner, S.J. Cuthbert, K. Mehta, P.J. O'Brien, The timing of stabilisation and the exhumation rate for ultra-high pressure rocks in the Western Gneiss Region of Norway, J. Metamorph. Geol. 21 (2003) 601–612.
[9] E.J. Krogh, D.A. Carswell, HP and UHP eclogites and garnet peridotites in the Scandinavian Caledonides, in: R.G. Coleman, X. Wang (Eds.), Ultrahigh Pressure Metamorphism, Cambridge University Press, Stanford, 1995, pp. 244–298.
[10] W.G. Ernst, Metamorphism, partial preservation, and exhumation of ultrahigh-pressure belts, Isl. Arc 8 (1999) 125–153.
[11] D. Gebauer, M.A. Lappin, M. Grunenfelder, A. Wyttenbach, The age and origin of some Norwegian eclogites: a U–Pb zircon and REE study, Chem. Geol. 52 (1985) 227–247.
[12] M.P. Terry, P. Robinson, M.A. Hamilton, M.J. Jercinovic, Monazite geochronology of UHP and HP metamorphism, deformation, and exhumation, Nordøyane, Western Gneiss Region, Norway, Am. Mineral. 85 (2000) 1651–1664.
[13] T.E. Krogh, B.O. Mysen, G.L. Davis, A Paleozoic age for the primary minerals of a Norwegian eclogite, Carnegie Inst, Wash. Yearb. 73 (1974) 575–576.
[14] D.A. Carswell, R.D. Tucker, P.J. O'Brien, T.E. Krogh, Coesite inclusions and the U/Pb age of zircons from the Hareidland Eclogite in the Western Gneiss Region of Norway, Lithos 67 (2003) 181–190.

[15] T.E. Krogh, P. Robinson, M.P. Terry, Precise U–Pb zircon ages define 18 and 19 m.y. subduction to uplift intervals in the Averøya-Nordøyane area, Western Gneiss Region, in: E.A. Eide (Ed.), The Alice Wain Memorial West Norway Eclogite Field Symposium, 2003, p. 71.
[16] U. Schärer, L. Labrousse, Dating the exhumation of UHP rocks and associated crustal melting in the Norwegian Caledonides, Contrib. Mineral. Petrol. 144 (2003) 758–770.
[17] J.M. Mattinson, Multi-step high-resolution Pb/U and Pb/Pb zircon age spectra: combined annealing, partial dissolution, and TIMS analysis, Eos Trans. AGU 82 (47) (2001) (Abst. V22C-1056).
[18] J.M. Mattinson, CA (chemical abrasion)-TIMS: high-resolution U–Pb zircon geochronology combining high-temperature annealing of radiation damage and multi-step partial dissolution analysis, Eos Trans. AGU 84 (46) (2003) (Abst. V22E-06).
[19] J.M. Mattinson, Zircon U–Pb chemical abrasion ("CA-TIMS") method: combined annealing and multi-step dissolution analysis for improved precision and accuracy of zircon ages, Chem. Geol. (in review).
[20] J.M. Mattinson, Analysis of zircon by multi-step partial dissolutions: the good, the bad, and the ugly, GAC/MAC Ottawa Abst. Vol., 1997, p. A98.
[21] F. Corfu, Extraction of Pb with artificially too-old ages during stepwise dissolution experiments on Archean zircon, Lithos 53 (2000) 279–291.
[22] D.W. Davis, T.E. Krogh, Preferential dissolution of 234U and radiogenic Pb from alpha-recoil-damaged lattice sites in zircon: implications for thermal histories and Pb isotopic fractionation in the near surface environment, Chem. Geol. 172 (2000) 41–58.
[23] F. Chen, W. Siebel, M. Satir, Zircon U–Pb and Pb-isotope fractionation during stepwise HF acid leaching and geochronological implications, Chem. Geol. 191 (2002) 155–164.
[24] S.S. Sun, W.F. McDonough, Chemical and isotopic systematics of oceanic basalts: implications for mantle composition and processes, in: A.D. Saunders, M.J. Norry (Eds.), Magmatism in the Ocean Basins, Geological Society of London Spec. Publ. 42 (1989) 313–345.
[25] A. Wain, D. Waters, A. Jephcoat, H. Olijynk, The high-pressure to ultrahigh-pressure transition in the Western Gneiss Region, Norway, Eur. J. Mineral 12 (2000) 667–687.
[26] I. Bryhni, W.L. Griffin, Zoning in eclogite garnets from Nordfjord, west Norway, Contrib. Mineral. Petrol. 32 (1971) 112–125.
[27] D.A. Carswell, S.J. Cuthbert, New insights on the petrological evolution of high-ultrahigh pressure eclogites in the Stadlandet-Nordfjord area of western Norway, in: E.A. Eide (Ed.), The Alice Wain Memorial West Norway Eclogite Field Symposium, 2003, pp. 29–30.
[28] K.P. Skjerlie, A.E. Patiño Douce, The fluid-absent partial melting of a zoisite-bearing quartz eclogite from 1.0 to 3.2 GPa; implications for melting in thickened continental crust and for subduction-zone processes, J. Petrol. 43 (2002) 291–314.
[29] W.L. Griffin, H.K. Brueckner, REE, Rb–Sr and Sm–Nd studies of Norwegian eclogites, Chem. Geol. 52 (1985) 249–271.
[30] D.B. Root, B.R. Hacker, P.B. Gans, M.N. Ducea, E.A. Eide, J.L. Mosenfelder, Discrete ultrahigh-pressure domains in the Western Gneiss Region, Norway: implications for formation and exhumation, Lithos (in review).
[31] P.W.O. Hoskin, L.P. Black, Metamorphic zircon formation by solid-state recrystallization of protolith igneous zircon, J. Metamorph. Geol. 18 (2000) 423–439.
[32] A.H. Jaffey, K.F. Flynn, L.E. Glendenin, W.C. Bentley, A.M. Essling, Precision measurement of half-lives and specific activities of 235U and 238U, Phys. Rev., C 4 (1971) 1889–1906.
[33] L.M. Heaman, A.N. LeCheminant, Anomalous U–Pb systematics in mantle-derived baddeleyite xenocrysts from Île Bizard: evidence for high-temperature diffusion? Chem. Geol. 172 (2001) 77–93.
[34] R. Anczkiewicz, F. Oberli, J.P. Burg, I.M. Villa, D. Günther, M. Meier, Timing of normal faulting along the Indus Suture in Pakistan Himalaya and a case of major 231Pa/235U initial disequilibrium in zircon, Earth Planet. Sci. Lett. 191 (2001) 101–114.
[35] P.W.O. Hoskin, T.R. Ireland, Rare earth element chemistry of zircon and its use as a provenance indicator, Geology 28 (2000) 627–630.
[36] U. Schaltegger, C.M. Fanning, D. Günther, J.C. Maurin, K. Schulmann, D. Gebauer, Growth, annealing and recrystallization of zircon and preservation of monazite in high-grade metamorphism: conventional and in-situ U–Pb isotope, cathodoluminescence and microchemical evidence, Contrib. Mineral. Petrol. 134 (1999) 186–201.
[37] D. Rubatto, Zircon trace element geochemistry: partitioning with garnet and the link between U–Pb ages and metamorphism, Chem. Geol. 184 (2002) 123–138.
[38] W. Sun, I.S. Williams, S. Li, Carboniferous and Triassic eclogites in the western Dabie Mountains, east-central China: evidence for protracted convergence of the North and South China Blocks, J. Metamorph. Geol. 20 (2002) 873–886.
[39] M.J. Whitehouse, J.P. Platt, Dating high-grade metamorphism—constraints from rare-earth elements in zircon and garnet, Contrib. Mineral. Petrol. 145 (2003) 61–74.
[40] B. Bingen, H. Austrheim, M.J. Whitehouse, W.J. Davis, Trace element signature and U–Pb geochronology of eclogite-facies zircon, Bergen Arcs, Caledonides of W Norway, Contrib. Mineral. Petrol. 147 (2004) 671–683.
[41] D.J. Cherniak, Pb diffusion in rutile, Contrib. Mineral. Petrol. 139 (2000) 198–207.
[42] M.D. Schmitz, S.A. Bowring, Constraints on the thermal evolution of continental lithosphere from U–Pb accessory mineral thermochronometry of lower crustal xenoliths, southern Africa, Contrib. Mineral. Petrol. 144 (2003) 592–618.
[43] E.O. Walsh, B.R. Hacker, The fate of subducted continental margins: two-stage exhumation of the high-pressure and ultrahigh-pressure Western Gneiss Region, Norway, J. Metamorph. Geol. 22 (2004) 671–687.